

## **Influence of Cerium (Ce) doping on the Optical properties of silver sulphide (Ag<sub>2</sub>S) and silver sulphide (Ce: Ag<sub>2</sub>S) thin films deposited by electrodeposition method.**

### **Abstract**

Thin Films of silver sulphide (Ag<sub>2</sub>S) have been successfully deposited onto FTO glass substrate using electrodeposition method to investigate the effects of Ce doping on Ag<sub>2</sub>S films. Silver trioxonitrate (V) and Sodium thiosulphate were the precursors used for silver and sulphur ions. Depositions of thin films made from cerium-doped silver sulphide were conducted at room temperature. Variations of percentage concentration of cerium dopant (2.5%, 5.0%, 7.5% and 10.0%) were considered in this paper. The optical properties of the thin films were characterized using Uv-Vis spectrometry. Absorbance results confirm that increasing Ce concentration significantly boosts the absorbance of Ag<sub>2</sub>S thin films, with the Ce: 10.0% film being the most effective in absorbing UV, visible, and near-infrared light, making it a strong candidate for applications in photovoltaics and optical devices, increasing Ce concentration results in reduced transmittance, making the films more absorptive, especially at higher concentrations, where Ce: 10.0% is the least transparent and most effective for applications requiring light absorption. Ce doping slightly increases the reflectance of Ag<sub>2</sub>S films, with higher Ce concentrations leading to higher reflectance, especially in the near-infrared region. This suggests that as Ce concentration increases, the films reflect more light, potentially reducing their effectiveness for absorption-based applications but increasing their suitability for applications where light reflection is desired. For extinction coefficient, the results revealed that the undoped Ag<sub>2</sub>S film shows the highest extinction coefficient, while doping with Ce generally reduces the extinction coefficient, with the 5.0% and 7.5% Ce-doped films exhibiting the lowest values. Other optical results were also presented.

**Key Words:** Silver Sulphide, optical properties, Optoelectronics, Electrodeposition

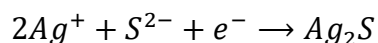
### **1. Introduction**

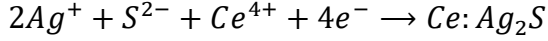
Silver sulphide ( $Ag_2S$ ) is an important member of the chalcogenides, which are compounds formed with chalcogen elements ( Group 16 elements in the periodic table, such as sulphur, selenium and tellurium) and metals. Silver sulphide is considered a binary chalcogenide because it consists of silver (Ag) and sulphur (S), a chalcogen element. Silver sulphide has notable properties that make it of interest in various scientific and technological fields, including electronics, materials science and chemistry. Silver sulphide exists mainly in two crystalline forms:- acanthite and argentite. Acanthite is stable at lower temperatures, while argentite is stable at higher temperatures. Silver sulphide is a fascinating chalcogenide material with a combination of useful electronic and structural properties, making it valuable in both research and industrial applications. Cerium (Ce) is commonly used as a dopant in various materials to modify their optical, electrical and catalytic properties. When cerium is introduced into a host material, such as silver sulphide, it can improve performance in specific applications. However, to the best of our knowledge, there are limited works that have been done in these material combinations. Hence, in this paper we report the influence of cerium (ce) doping on the optical properties of silver sulphide ( $Ag_2S$ ) and silver sulphide (Ce:  $Ag_2S$ ) thin films deposited by electrodeposition method at different percentage molar concentration [1]

## 2. Experimental

### 2.1. Electrodeposition of silver sulphide ( $Ag_2S$ ) and cerium doped silver sulphide (Ce: $Ag_2S$ ) thin films

For electrodeposition of silver sulphide thin film on FTO substrate, aqueous electrolytic bath composed of 20 ml of 0.05M of silver trioxonitrate (V) was used to dissolve 0.7 g of EDTA to form complex solution. After stirring for 5 minutes, 20 ml of 0.05M of sodium thiosulphate was added to the solution. The mixture was stirred for another 10 minute to totally dissolve the EDTA. The three electrodes were immersed into the bath containing the electrolytic solution and 1.5 volts was allowed to pass through the setup for 120 seconds (2 minutes). After the allowed time, dark film of  $Ag_2S$  was found to be deposited on the conductive surface of the FTO substrate. The deposited  $Ag_2S$  thin film was heat-treated at 100 °C for 10 minute to remove water and increase the crystallinity of the deposited thin film. The mechanism of the formation of silver sulphide and cerium doped silver sulphide is shown in equation (1) and (2).





2

## 2.2. Optimization of Ce ion concentration for Ce: Ag<sub>2</sub>S thin films

For the deposition of Ce doped Ag<sub>2</sub>S thin films, 0.05 M of cerium (IV) tetraoxosulphatetetrahydrate was used. Similar procedure used for deposition of silver sulphidethin film was adopted but with addition of different volume concentrations of 0.05 M of cerium (IV) tetraoxosulphatetetrahydrate as shown in Table 1. Four samples with different dopant volume concentrations of 1 ml, 2 ml, 3 ml and 4 ml were fabricated.

**Table 1: Bath parameter for deposition of Ag<sub>2</sub>S and Ce doped Ag<sub>2</sub>S thin films**

0.05 M of AgNO <sub>3</sub>	0.05 M of Na <sub>2</sub> S <sub>2</sub> O <sub>3</sub>	0.05 M of CeSO <sub>4</sub> ·4H <sub>2</sub> O	EDTA	Applied Voltage	Time
Vol. (ml)	Vol. (ml)	Vol. (ml)	Conc. (g)	(volts)	(sec.)
20.00	20.00	-	0.70	1.50	120
20.00	20.00	1.00	0.70	1.50	120
20.00	20.00	2.00	0.70	1.50	120
20.00	20.00	3.00	0.70	1.50	120
20.00	20.00	4.00	0.70	1.50	120

## 2.3. Optical characterization

The optical absorbance of the films deposited was obtained using spectrophotometer (model: 756S UV – VIS). Other optical properties of the films such as transmittance, reflectance, refractive index, extinction coefficient, real dielectric constant, imaginary dielectric constant and energy band gap were evaluated using the formulae below;

Transmittance of the film was evaluated using equation (3) given by [1, 2]

$$T = 10^{-A} \quad 3$$

Reflectance was obtained using the expression in equation (4) as given by [3, 4, 5].

$$R = 1 - [T \cdot \exp \exp(A)]^{\frac{1}{2}} \quad 4$$

The absorption coefficient ( $\alpha$ ) was calculated from the transmittance values using the equation (5) as given by [6, 7, 8].

$$\alpha = \frac{1}{t} \left( \frac{1}{T} \right). \quad 5$$

Where  $t$  is the thickness of the film obtained using equation (3) above.

Extinction coefficient was obtained using equation (6) as given by [9, 10, 11].

$$k = \frac{\alpha \lambda}{4\pi} \quad 6$$

Refractive indices of the films were calculated using equation (7) as given by [3, 12, 13].

$$\eta = \frac{1+R}{1-R} + \sqrt{\frac{4R}{(1-R)^2} - k^2} \quad 7$$

Optical conductivity was estimated using equation (8) as given by [14, 15, 16].

$$\sigma_o = \frac{\alpha \eta c}{4\pi}. \quad 8$$

Where  $c$  is the speed of light.

The energy band gap was estimated using Tauc's model of equation (9) as given by [9, 17]

$$(\alpha h\nu)^n = \beta(h\nu - E_g). \quad 9$$

Where  $\beta$  is a constant,  $n = 2$  for direct band gap. The energy band gaps of the films were obtained by extrapolating the straight portion of the plot of  $(\alpha h\nu)^2$  against the photon energy  $(h\nu)$  at  $(\alpha h\nu)^2 = 0$ .

### 3. Results and discussion

#### (3.1) Optical properties of Ag<sub>2</sub>S with variation of percentage concentration of cerium dopant

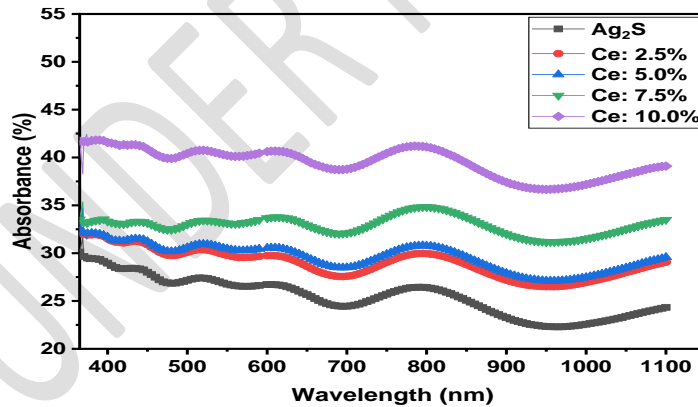


Figure 1: Plot of absorbance against wavelength for cerium doped silver sulphide thin films deposited at different concentration of cerium ion precursor

Figure 1 showed the plot of absorbance against wavelength for silver sulphide and cerium doped silver sulphide thin films deposited at different concentration of cerium ion precursor. The absorbance of Ag<sub>2</sub>S and Ce-doped silver sulphide (Ce:Ag<sub>2</sub>S) thin films varies significantly

across different wavelengths, with Ce doping consistently enhancing absorbance as the concentration increases. The undoped  $\text{Ag}_2\text{S}$  film exhibits the lowest absorbance, with values of 30.12% at 365 nm, 28.95% at 400 nm, 24.45% at 700 nm, and 24.33% at 1100 nm, showing a gradual decline with increasing wavelength. In contrast, the Ce-doped films demonstrate higher absorbance, starting with Ce: 2.5%, which shows improved values of 32.38%, 31.53%, 27.58%, and 29.06% at the respective wavelengths. The Ce: 5.0% film further increases absorbance to 32.56%, 31.69%, 28.50%, and 29.57%, particularly in the UV and visible regions. The Ce: 7.5% film continues this trend with absorbance values of 33.54%, 33.32%, 32.09%, and 33.50%, indicating significant improvement across the visible and near-infrared regions. The Ce: 10.0% film exhibits the highest absorbance values of 41.72%, 41.58%, 38.79%, and 39.10%, showing a substantial enhancement across the entire spectrum. These results confirm that increasing Ce concentration significantly boosts the absorbance of  $\text{Ag}_2\text{S}$  thin films, with the Ce: 10.0% film being the most effective in absorbing UV, visible, and near-infrared light, making it a strong candidate for applications in photovoltaics and optical devices.

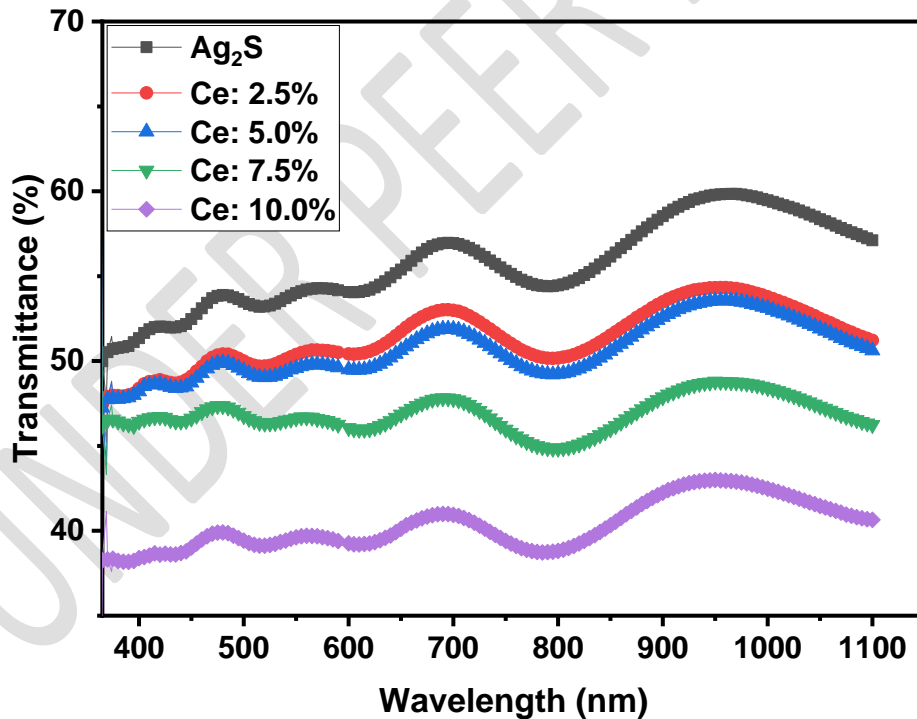


Figure 2: Plot of transmittance against wavelength for cerium doped silver sulphide thin films deposited at different concentration of cerium ion precursor

Figure 2 showed the plot of transmittance against wavelength for silver sulphide and cerium doped silver sulphide thin films deposited at different concentration of cerium ion precursor. The transmittance of  $\text{Ag}_2\text{S}$  and Ce-doped  $\text{Ag}_2\text{S}$  thin films shows a clear decreasing trend as the concentration of cerium increases across the UV, visible, and near-infrared regions. The undoped  $\text{Ag}_2\text{S}$  film exhibits the highest transmittance, with values of 49.99% at 365 nm, 51.34% at 400 nm, 56.94% at 700 nm, and 57.11% at 1100 nm, indicating high transparency. In contrast, the Ce-doped films progressively show reduced transmittance as Ce concentration increases. For Ce: 2.5%, transmittance decreases slightly to 47.45% at 365 nm, 48.38% at 400 nm, 52.99% at 700 nm, and 51.22% at 1100 nm. This trend continues with Ce: 5.0%, with values of 47.25%, 48.21%, 51.88%, and 50.62%, showing more light absorption. Ce: 7.5% shows a more pronounced decrease, with transmittance of 46.19%, 46.43%, 47.76%, and 46.24%, indicating significantly reduced transparency. Finally, Ce: 10.0% exhibits the lowest transmittance, with values of 38.26%, 38.39%, 40.94%, and 40.64%, demonstrating a substantial reduction in light transmission and increased absorption across all regions. The increasing Ce concentration results in reduced transmittance, making the films more absorptive, especially at higher concentrations, where Ce: 10.0% is the least transparent and most effective for applications requiring light absorption.

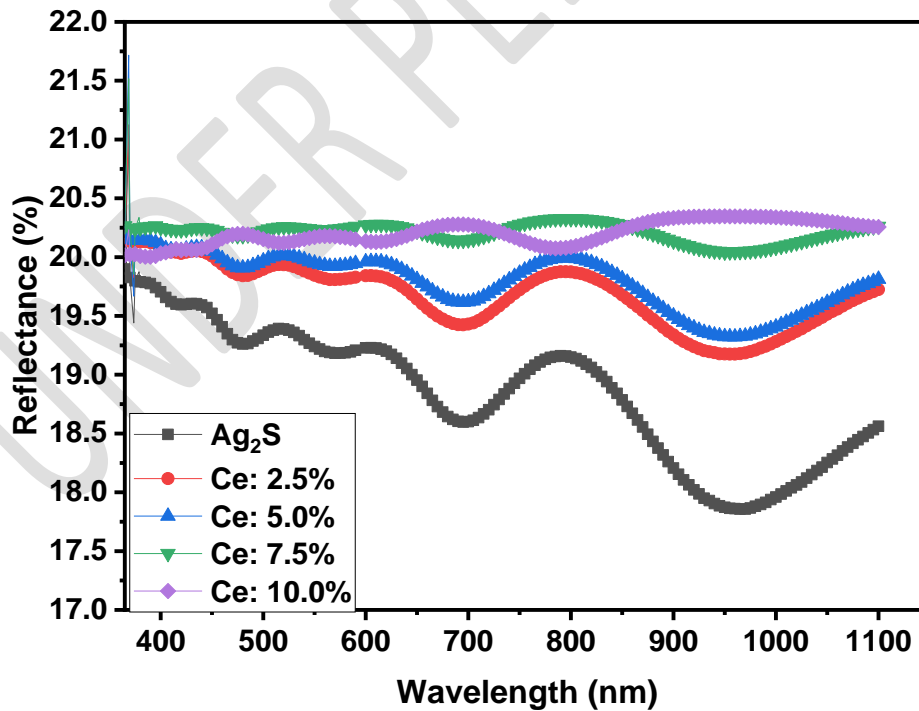


Figure 3: Plot of reflectance against wavelength for cerium doped silver sulphide thin films deposited at different concentration of cerium ion precursor

Figure 3 showed the plot of reflectance against wavelength for silver sulphide and cerium doped silver sulphide thin films deposited at different concentration of cerium ion precursor. The reflectance data for undoped  $\text{Ag}_2\text{S}$  and Ce-doped  $\text{Ag}_2\text{S}$  thin films, across the UV (365–400 nm), visible (400–700 nm), and near-infrared (700–1100 nm) regions, reveal subtle variations with increasing Ce concentration. The undoped  $\text{Ag}_2\text{S}$  film shows the lowest reflectance values, starting at 19.90% at 365 nm, 19.71% at 400 nm, 18.60% at 700 nm, and 18.56% at 1100 nm, indicating relatively low light reflection. For Ce: 2.5%, the reflectance increases slightly across all regions, with values of 20.17%, 20.09%, 19.43%, and 19.72%, reflecting more light compared to the undoped sample. The reflectance for Ce: 5.0% continues this trend, with values of 20.19%, 20.10%, 19.62%, and 19.81%, showing a gradual increase in reflection. The Ce: 7.5% film shows a further increase, especially in the visible and near-infrared regions, with values of 20.26%, 20.25%, 20.15%, and 20.26%. Lastly, the Ce: 10.0% film exhibits the highest reflectance, with values of 20.01%, 20.03%, 20.27%, and 20.26%, showing a consistent increase across the spectrum. From the results obtained, Ce doping slightly increases the reflectance of  $\text{Ag}_2\text{S}$  films, with higher Ce concentrations leading to higher reflectance, especially in the near-infrared region. This suggests that as Ce concentration increases, the films reflect more light, potentially reducing their effectiveness for absorption-based applications but increasing their suitability for applications where light reflection is desired.

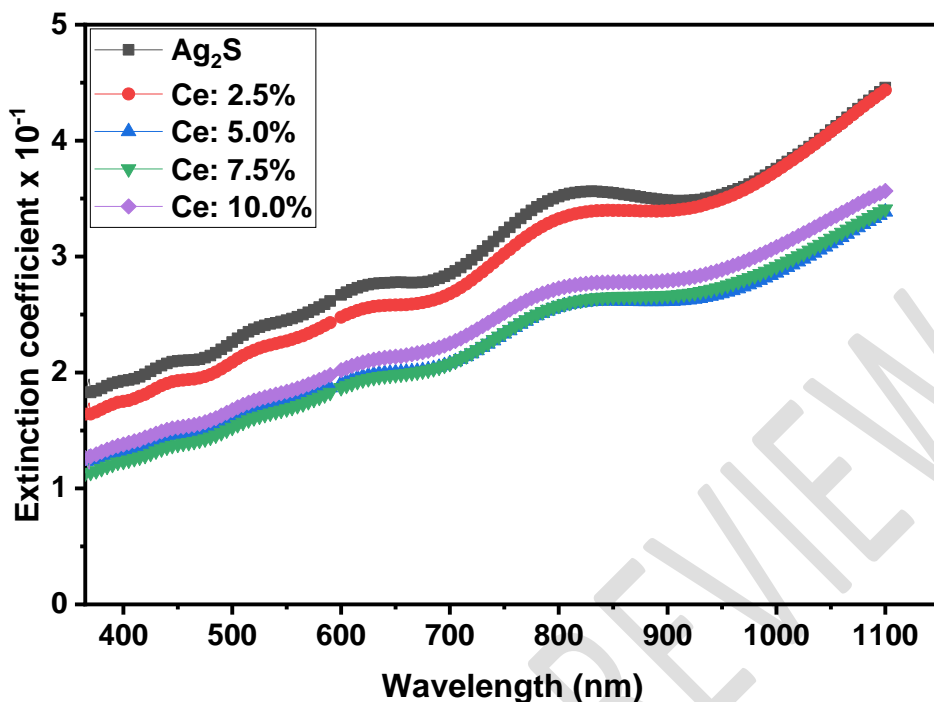


Figure 4: Plot of extinction coefficient against wavelength for cerium doped silver sulphide thin films deposited at different concentration of cerium ion precursor

Figure 4 showed the plot of extinction coefficient against wavelength for silver sulphide and cerium doped silver sulphide thin films deposited at different concentration of cerium ion precursor. The extinction coefficient values for Ag<sub>2</sub>S and Ce-doped Ag<sub>2</sub>S thin films across different Ce concentrations provide insight into how light is absorbed by the material as it propagates through it. For the undoped Ag<sub>2</sub>S film, the extinction coefficient starts at  $1.83 \times 10^{-1}$  at 365 nm, increases to  $1.93 \times 10^{-1}$  at 400 nm,  $2.85 \times 10^{-1}$  at 700 nm, and peaks at  $4.46 \times 10^{-1}$  at 1100 nm, indicating significant absorption, particularly in the near-infrared region. For Ce: 2.5%, the extinction coefficient slightly decreases, with values of  $1.64 \times 10^{-1}$  at 365 nm,  $1.75 \times 10^{-1}$  at 400 nm,  $2.68 \times 10^{-1}$  at 700 nm, and  $4.44 \times 10^{-1}$  at 1100 nm, suggesting reduced absorption compared to the undoped film. As the Ce concentration increases to Ce: 5.0%, the extinction coefficient further decreases, with values of  $1.24 \times 10^{-1}$ ,  $1.32 \times 10^{-1}$ ,  $2.08 \times 10^{-1}$ , and  $3.39 \times 10^{-1}$ , reflecting even lower absorption. For Ce: 7.5%, the extinction coefficient remains relatively low, with values of  $1.13 \times 10^{-1}$  at 365 nm,  $1.23 \times 10^{-1}$  at 400 nm,  $2.08 \times 10^{-1}$  at 700 nm, and  $3.41 \times 10^{-1}$  at 1100 nm, continuing the trend of reduced absorption. Finally, for Ce: 10.0%, the extinction coefficient increases slightly compared

to the 7.5% film, with values of  $1.26 \times 10^{-1}$ ,  $1.38 \times 10^{-1}$ ,  $2.25 \times 10^{-1}$ , and  $3.57 \times 10^{-1}$ , suggesting improved absorption at higher Ce concentrations, particularly in the near-infrared region. The results revealed that the undoped  $\text{Ag}_2\text{S}$  film shows the highest extinction coefficient, while doping with Ce generally reduces the extinction coefficient, with the 5.0% and 7.5% Ce-doped films exhibiting the lowest values. However, the 10.0% Ce-doped film shows a slight increase, indicating that at higher Ce concentrations, absorption properties improve again.

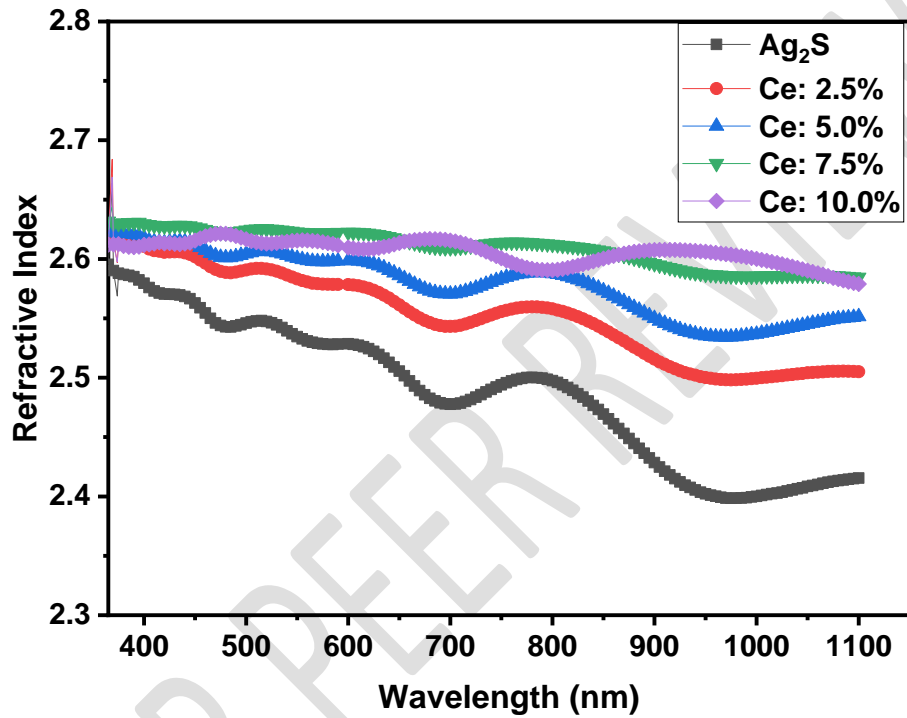


Figure 5: Plot of refractive index against wavelength for cerium doped silver sulphide thin films deposited at different concentration of cerium ion precursor

Figure 5 showed the plot of refractive index against wavelength for silver sulphide and cerium doped silver sulphide thin films deposited at different concentration of cerium ion precursor. The refractive index values for  $\text{Ag}_2\text{S}$  and Ce-doped  $\text{Ag}_2\text{S}$  thin films across different Ce concentrations demonstrate how light is slowed down in these materials as it travels through them. For the undoped  $\text{Ag}_2\text{S}$  film, the refractive index starts at 2.60 at 365 nm, decreases to 2.58 at 400 nm, 2.48 at 700 nm, and further drops to 2.42 at 1100 nm, indicating a decline in the refractive index as the wavelength increases. For Ce: 2.5%, the refractive index values slightly increase compared to the undoped film, with values of 2.62 at 365 nm, 2.61 at 400 nm, 2.54 at 700 nm, and 2.51 at 1100 nm, suggesting a more stable refractive behavior across the spectrum. The Ce: 5.0% film continues this increasing trend, with values of 2.63, 2.62, 2.57, and 2.55,

indicating higher refractive indices across all wavelengths, which implies improved light-matter interaction. For Ce: 7.5%, the refractive index values further increase to 2.63 at 365 nm, 2.63 at 400 nm, 2.61 at 700 nm, and 2.58 at 1100 nm, highlighting the enhancing effect of higher Ce doping levels on refractive properties. The Ce: 10.0% film shows similar values, with 2.61 at 365 nm, 2.61 at 400 nm, 2.62 at 700 nm, and 2.58 at 1100 nm, indicating that the refractive index remains relatively high at higher Ce concentrations. From the results, Ce doping resulted in an increase in the refractive index of  $\text{Ag}_2\text{S}$  thin films, with the effect becoming more pronounced at higher Ce concentrations. This increase in refractive index suggests that Ce-doped films exhibit improved optical density, which could be beneficial for applications that require higher refractive materials, such as in photonic devices or optical coatings.

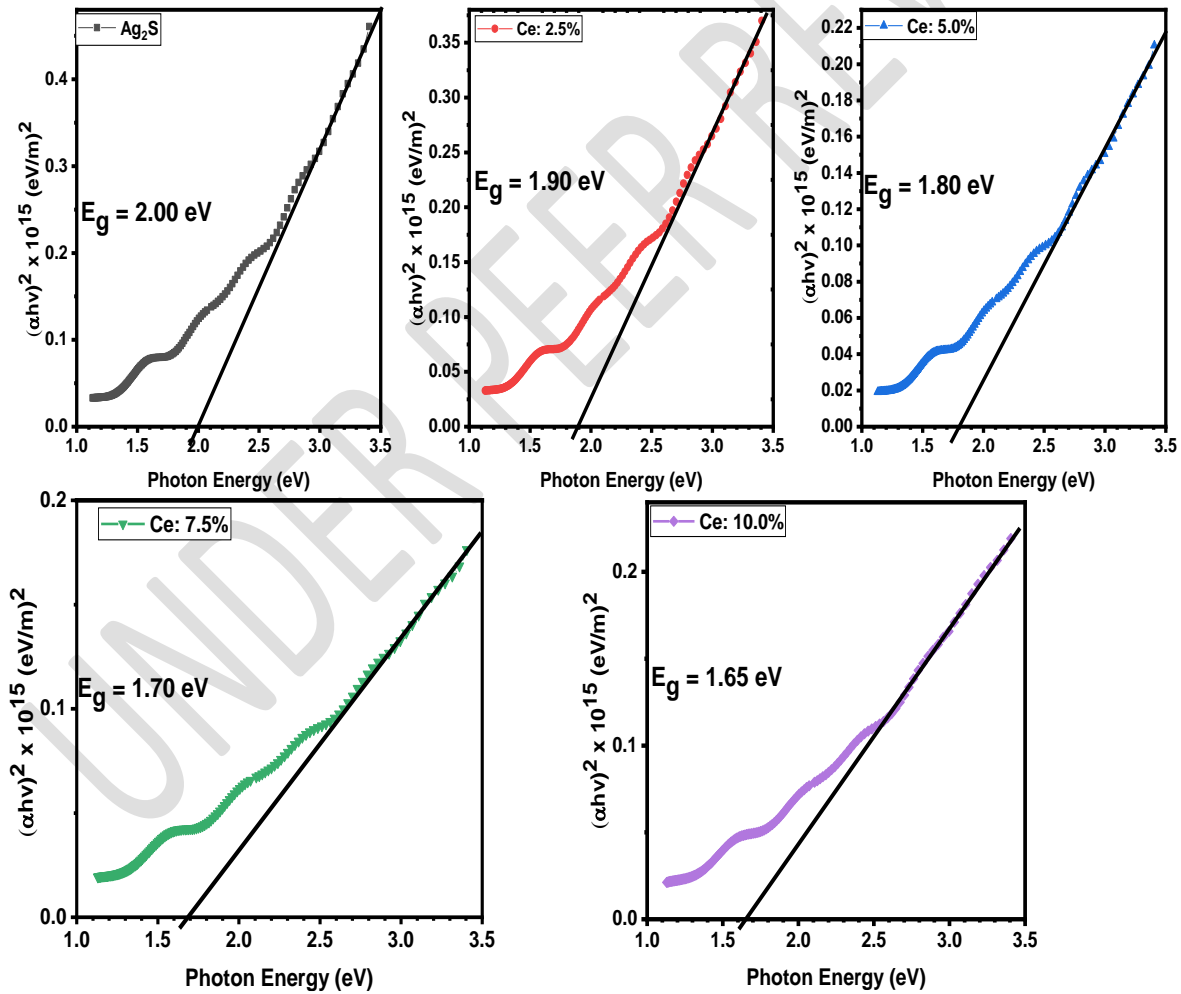


Figure 6: Plot of  $(\alpha h\nu)^2$  against photon energy for cerium doped silver sulphide thin films deposited at different concentration of cerium ion precursor

Figure 6 shows the plot of  $(ahv)^2$  versus photon energy for  $\text{Ag}_2\text{S}$  and Ce-doped  $\text{Ag}_2\text{S}$  thin films at different Ce concentrations, from which the energy band gaps were estimated by extrapolating the linear portion of each graph along the photon energy axis where  $(ahv)^2$  equals zero. For undoped  $\text{Ag}_2\text{S}$ , the energy band gap was determined to be 2.00 eV. As the Ce concentration increased, the band gap decreased, with Ce: 2.5%, 5.0%, 7.5%, and 10.0% showing band gaps of 1.90 eV, 1.80 eV, 1.70 eV, and 1.65 eV, respectively. This trend indicates that Ce doping effectively reduces the energy band gap of  $\text{Ag}_2\text{S}$  thin films, enhancing their optical absorption capabilities and making them more suitable for applications requiring efficient light absorption, such as solar energy harvesting and optoelectronic devices. The obtained band gap of silver sulphide is within band gap range of 2.10 to 2.2 eV reported by [19] and 2.01 to 2.23 eV obtained by [20]. The decrease in band gap consistent with previous studies that have reported band gap narrowing due to the introduction of impurity energy levels within the band structure of doped semiconductors [21, 22].

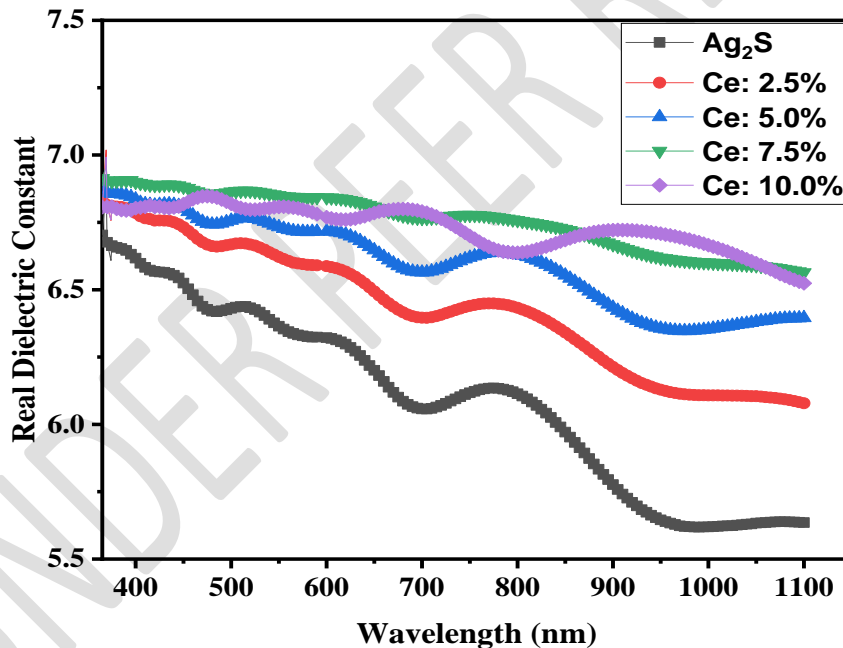


Figure 7: Plot of real dielectric constant against wavelength for cerium doped silver sulphide thin films deposited at different concentration of cerium ion precursor

Figure 7 showed the plot of real dielectric constant against wavelength for silver sulphide and cerium doped silver sulphide thin films deposited at different concentration of cerium ion precursor. The real dielectric constant ( $\epsilon_r$ ) of  $\text{Ag}_2\text{S}$  and Ce-doped  $\text{Ag}_2\text{S}$  thin films shows an overall increase with increasing Ce concentration, indicating enhanced optical energy storage

capabilities. For the undoped  $\text{Ag}_2\text{S}$ , the real dielectric constant starts at 6.70 at 365 nm and decreases gradually to 5.64 at 1100 nm, suggesting reduced dielectric properties at longer wavelengths. In contrast, the Ce-doped films exhibit progressively higher dielectric constants compared to the undoped film, with Ce: 2.5%, 5.0%, 7.5%, and 10.0% showing improvements across the wavelength range, reaching up to 6.83, 6.88, 6.91, and 6.81 at 365 nm, respectively. The highest values are observed for the Ce: 7.5% film, with a real dielectric constant of 6.91 at 365 nm and 6.56 at 1100 nm, indicating that doping with Ce enhances the dielectric properties, especially at intermediate concentrations. The results suggest that Ce doping effectively improves the dielectric constant of  $\text{Ag}_2\text{S}$  thin films, enhancing their potential for use in electronic and optoelectronic devices where higher dielectric properties are advantageous.

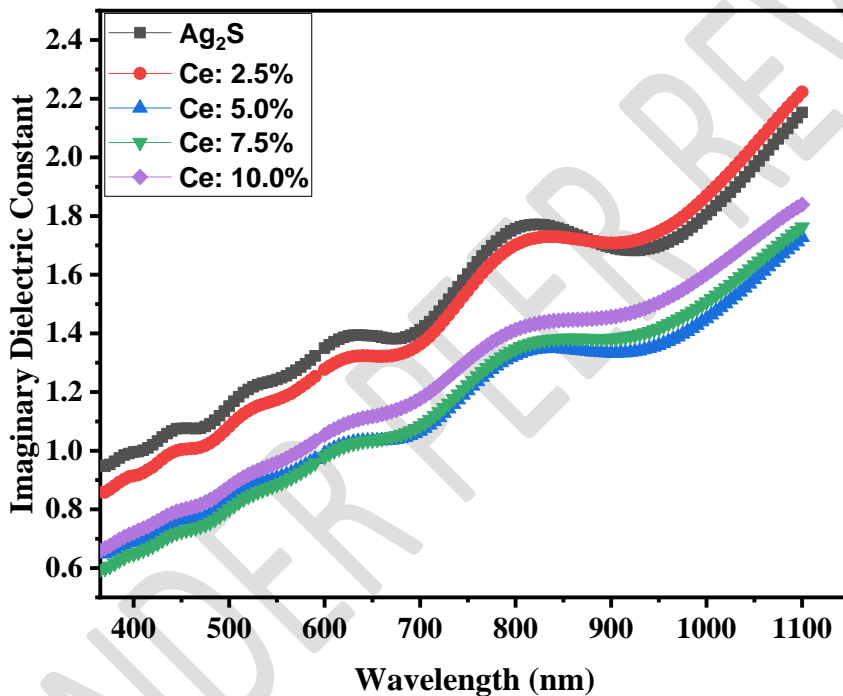


Figure 8: Plot of imaginary dielectric constant against wavelength for cerium doped silver sulphide thin films deposited at different concentration of cerium ion precursor

Figure 8 showed the plot of imaginary dielectric against wavelength for silver sulphide and cerium doped silver sulphide thin films deposited at different concentration of cerium ion precursor. The imaginary dielectric constant  $\epsilon_i$  of  $\text{Ag}_2\text{S}$  and Ce-doped  $\text{Ag}_2\text{S}$  thin films provides insight into the material's optical loss properties. For the undoped  $\text{Ag}_2\text{S}$  film, the imaginary dielectric constant starts at 0.95 at 365 nm, increases to 0.99 at 400 nm, further rises to 1.41 at 700 nm, and reaches 2.15 at 1100 nm, indicating an increasing trend in energy loss as the

wavelength increases. For Ce: 2.5%, the imaginary dielectric constant is slightly lower across all wavelengths compared to the undoped film, with values of 0.86, 0.91, 1.36, and 2.22 at 365 nm, 400 nm, 700 nm, and 1100 nm, respectively, suggesting a moderate reduction in energy dissipation. The Ce: 5.0% film shows a further reduction in the imaginary dielectric constant, with values of 0.65, 0.69, 1.07, and 1.73, indicating a significant reduction in energy loss, especially at shorter wavelengths. For Ce: 7.5%, the imaginary dielectric constant values are 0.60 at 365 nm, 0.65 at 400 nm, 1.08 at 700 nm, and 1.76 at 1100 nm, continuing the trend of reduced energy dissipation compared to undoped  $\text{Ag}_2\text{S}$ . Finally, for Ce: 10.0%\*\*, the imaginary dielectric constant increases slightly, with values of 0.66, 0.72, 1.18, and 1.84, indicating a slight increase in energy loss at higher Ce concentrations, particularly in the near-infrared region. Ce doping of  $\text{Ag}_2\text{S}$  generally reduces the imaginary dielectric constant of the thin films, suggesting a decrease in energy dissipation, with the lowest values observed for the 5.0% and 7.5% Ce-doped films, which could be beneficial for applications requiring minimal energy loss, such as in optoelectronic devices and solar cells.

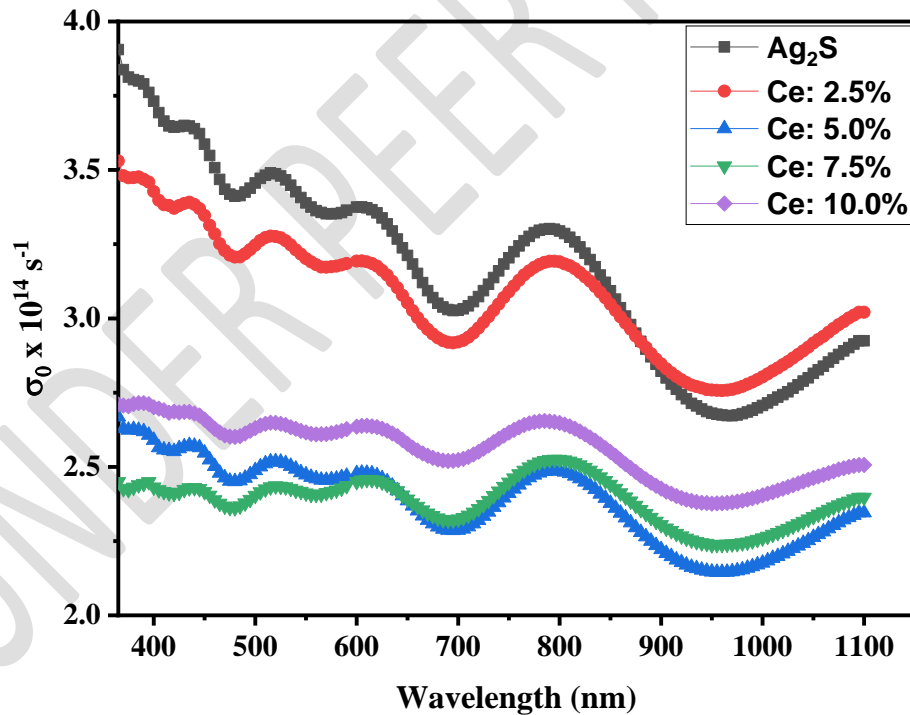


Figure 9: Plot of optical conductivity against wavelength for cerium doped silver sulphide thin films deposited at different concentration of cerium ion precursor

Figure 9 showed the plot of optical conductivity against wavelength for silver sulphide and cerium doped silver sulphide thin films deposited at different concentration of cerium ion precursor. The optical conductivity  $\sigma_o$  values for  $\text{Ag}_2\text{S}$  and Ce-doped  $\text{Ag}_2\text{S}$  thin films show notable variations across different Ce concentrations and wavelength ranges, highlighting the effect of cerium doping on the optical properties of these films. For the undoped  $\text{Ag}_2\text{S}$  film, the optical conductivity is highest, starting at  $3.91 \times 10^{14} \text{ s}^{-1}$  at 365 nm, decreasing to  $3.73 \times 10^{14} \text{ s}^{-1}$  at 400 nm,  $3.03 \times 10^{14} \text{ s}^{-1}$  at 700 nm, and dropping to  $2.92 \times 10^{14} \text{ s}^{-1}$  at 1100 nm, indicating a general decrease in optical conductivity with increasing wavelength. For Ce: 2.5%, the optical conductivity slightly decreases compared to the undoped film, with values of  $3.53 \times 10^{14} \text{ s}^{-1}$  at 365 nm,  $3.43 \times 10^{14} \text{ s}^{-1}$  at 400 nm,  $2.92 \times 10^{14} \text{ s}^{-1}$  at 700 nm, and an increase to  $3.02 \times 10^{14} \text{ s}^{-1}$  at 1100 nm, suggesting a moderate enhancement of optical conductivity in the near-infrared region. The Ce: 5.0% film shows a significant reduction in optical conductivity, with values of  $2.67 \times 10^{14} \text{ s}^{-1}$ ,  $2.59 \times 10^{14} \text{ s}^{-1}$ ,  $2.29 \times 10^{14} \text{ s}^{-1}$ , and  $2.35 \times 10^{14} \text{ s}^{-1}$  at 365 nm, 400 nm, 700 nm, and 1100 nm, respectively, indicating a reduction in optical response possibly due to a decrease in free charge carriers. For Ce: 7.5%, the optical conductivity values further decrease to  $2.45 \times 10^{14} \text{ s}^{-1}$ ,  $2.43 \times 10^{14} \text{ s}^{-1}$ ,  $2.32 \times 10^{14} \text{ s}^{-1}$ , and  $2.40 \times 10^{14} \text{ s}^{-1}$ , continuing the trend of reduced optical response. However, for Ce: 10.0%, the optical conductivity increases again to  $2.71 \times 10^{14} \text{ s}^{-1}$ ,  $2.70 \times 10^{14} \text{ s}^{-1}$ ,  $2.52 \times 10^{14} \text{ s}^{-1}$ , and  $2.51 \times 10^{14} \text{ s}^{-1}$ , particularly in the visible and near-infrared regions, indicating a partial recovery in optical properties. The results revealed that the introduction of Ce doping reduces the optical conductivity of  $\text{Ag}_2\text{S}$  thin films, with the highest reduction observed for the 5.0% and 7.5% concentrations, while a slight recovery is noted at 10.0%. This trend suggests that Ce doping influences the carrier concentration thereby impacting the material's ability to conduct optical energy, which could affect their potential applications in optoelectronic devices.

#### 4. Conclusion

The results of the optical investigation of silver sulphide and cerium doped silver sulphide thin films with different percentage concentration of cerium dopant showed the influence of cerium dopant on the optical properties of the electrodeposited thin films. Absorbance results confirm that increasing Ce concentration significantly boosts the absorbance of  $\text{Ag}_2\text{S}$  thin films, with the Ce: 10.0% film being the most effective in absorbing UV, visible, and near-infrared light, making it a strong candidate for applications in photovoltaics and optical devices. increasing Ce

concentration results in reduced transmittance, making the films more absorptive, especially at higher concentrations, where Ce: 10.0% is the least transparent and most effective for applications requiring light absorption. Ce doping slightly increases the reflectance of Ag<sub>2</sub>S films, with higher Ce concentrations leading to higher reflectance, especially in the near-infrared region. This suggests that as Ce concentration increases, the films reflect more light, potentially reducing their effectiveness for absorption-based applications but increasing their suitability for applications where light reflection is desired. For extinction coefficient, the results revealed that the undoped Ag<sub>2</sub>S film shows the highest extinction coefficient, while doping with Ce generally reduces the extinction coefficient, with the 5.0% and 7.5% Ce-doped films exhibiting the lowest values. However, the 10.0% Ce-doped film shows a slight increase, indicating that at higher Ce concentrations, absorption properties improve again. Ce doping resulted in an increase in the refractive index of Ag<sub>2</sub>S thin films, with the effect becoming more pronounced at higher Ce concentrations. This increase in refractive index suggests that Ce-doped films exhibit improved optical density, which could be beneficial for applications that require higher refractive materials, such as in photonic devices or optical coatings. Ce doping effectively reduces the energy band gap of Ag<sub>2</sub>S thin films, enhancing their optical absorption capabilities and making them more suitable for applications requiring efficient light absorption, such as solar energy harvesting and optoelectronic devices. The obtained band gap of silver sulphide is within band gap range of 2.10 to 2.2 eV reported by (Agbo and Nwofe, 2015) and 2.01 to 2.23 eV obtained by (Adelifard and Torkamani, 2015). The decrease in band gap consistent with previous studies that have reported band gap narrowing due to the introduction of impurity energy levels within the band structure of doped semiconductors (Pacheco-Salazar *et al.*, 2020; Liang *et al.*, 2017; Cheng *et al.*, 2016). It could also be seen from the result that Ce doping effectively improves the dielectric constant of Ag<sub>2</sub>S thin films, enhancing their potential for use in electronic and optoelectronic devices where higher dielectric properties are advantageous. Ce doping of Ag<sub>2</sub>S generally reduces the imaginary dielectric constant of the thin films, suggesting a decrease in energy dissipation, with the lowest values observed for the 5.0% and 7.5% Ce-doped films, which could be beneficial for applications requiring minimal energy loss, such as in optoelectronic devices and solar cells. The results revealed that the introduction of Ce doping reduces the optical conductivity of Ag<sub>2</sub>S thin films, with the highest reduction observed for the 5.0% and 7.5% concentrations, while a slight recovery is noted at 10.0%. This trend suggests that

Ce doping influences the carrier concentration thereby impacting the material's ability to conduct optical energy, which could affect their potential applications in optoelectronic devices.

## 7. References

1. Chukwudi Benjamin MUOMELIRI, Ngozi Agatha OKEREKE, Augustine Nwode NWORI, Uchechukwu Vincent OKPALA and Nonso Livinus OKOLI (2024), Electrosynthesis and Characterizations of Aluminum Silver Selenide ( $\text{AlAgSe}_2$ ), Thin Films for Possible Device Applications, international journal of research and scientific innovation, volume xi, issue ix
2. Lokhande, C. D., Sankapal, B. R., Mane, R. S., Pathan, H. M., Muller, M., Giersig, M. and Ganesan, V. (2002). XRD, SEM, AFM, HRTEM, EDAX and RBS studies of chemically deposited  $\text{Sb}_2\text{S}_3$  and  $\text{Sb}_2\text{Se}_3$  thin films. *Applied Surface Science*, 193(1), 1 – 10.
3. Ismail, B., Mushtaq, S. and Khan A. (2014). Enhanced Grain Growth in the Sn Doped  $\text{Sb}_2\text{S}_3$  Thin Film Absorber Materials for Solar Cell Applications. *Chalcogenide Letters*, 11(1), 37 – 45.
4. Augustine, C., Nwabuchi, M. N., Chikwenze, R. A., Anyaegbunam, F. N. C., Kalu, P. N., Robert, B. J., Nwosu, C. N., Dike, C. O. and Taddy, E. N. (2019). Comparative investigation of some selected properties of  $\text{Mn}_3\text{O}_4/\text{PbS}$  and  $\text{CuO}/\text{PbS}$  composites thin films. *Material Research Express*, 6 (066416), 1 – 10.
5. Guneri, E., (2019). The Role of Au Doping on the Structural and Optical Properties of  $\text{Cu}_2\text{O}$  Films. *Journal of Nano Research*, 58, 49 – 67.
6. Murali, D. S. and Aryasomayajula, S. (2018). Thermal conversion of  $\text{Cu}_4\text{O}_3$  into  $\text{CuO}$  and  $\text{Cu}_2\text{O}$  and the electrical properties of magnetron sputtered  $\text{Cu}_4\text{O}_3$  thin films. *Applied Physics A: Materials Science and Processing*, 124 (3), 1 – 7.
7. Suresh Sagadevan and Isha Das (2017). Chemical bath deposition (CBD) of zinc selenide ( $\text{ZnSe}$ ) thin films and characterization. *Australian Journal of Mechanical Engineering*, 15(3); 222 – 227.
8. Bekkari, R., Jaber, B., Labrim, H., Quafi, M., Zayyoun, N. and Laahab, L. (2019) Effect of Solvents and Stabilizer Molar Ratio on the Growth Orientation of Sol – Gel Derived ZnO Thin Films. *International Journal of Photoenergy*, 2019(3164043), 1 – 7.
9. Abouda, A. A., Mukherjeeb, A., Revaprasaduc, N. and Mohamed, A. N. (2019). The effect of Cu-doping on  $\text{CdS}$  thin films deposited by the spray pyrolysis technique. *Journal of Material Research and Technology*, 8(2):2021–2030.
10. Tezel, F. M., Ozdemir, O. and Kariper, I. A. (2017). The Effects of pH on Structural and Optical Characterization of Iron oxide Thin Films. *Surface Review and Letters*, 24(4), 1750051: 1 – 10.

11. Ongwen, N. O., Oduor, A. O. and Ayieta, E. O. (2019). Effect of Concentration of Reactants on the Optical Properties of Iron – Doped Cadmium Stannate Thin Films Deposited by Spray Pyrolysis. *American Journal of Materials Science*, 9(1): 1-7.
12. Sreedev, P., Rakesh, V. and Roshina N. S., (2018). Optical Characterization of ZnO thin Films Prepared by Chemical Bath Deposition Method. *IOP Conf. Series: Materials Science and Engineering*, 377(012086): 1 – 7.
13. Guneri, E. and Kariper, A. (2013). Characterization of high quality Chalcogenide thin films fabricated by Chemical Bath Deposition. *Electronic Materials Letters*, 9(1), 13 – 17.
14. Kariper, I. A. (2018). A new Route to Synthesis MnSe Thin films by Chemical Bath Method. *Material Research*, 21(2), 1 – 6.
15. Mahrov, B., Boschloo, G., Hgfeldt, A., Dloczuk, L. and Dittrich, T., (2004), Photovoltage Study of Charge Injection from Dye Molecules into Transparent Hole and Electron Conductors, *Applied Physics Letters*, 84(26), 5455 – 5457.
16. Mushtaq, S., Ismail, B., Raheel, M. and Zeb, A. (2016). Nickel Antimony Sulphide Thin Films for Solar Cell Application: Study of Optical Constants. *Natural Science*, 8, 33-40.
17. Ohwofosirai, A., Femi, M. D., Nwokike, A. N., Toluchi, O. J., Osuji, R. U. and Ezekoye, B. A. (2014). Study of the Optical Conductivity, Extinction Coefficient and Dielectric Function of CdO by Successive Ionic Layer Adsorption and Reaction (SILAR) Techniques. *American Chemical Science Journal*, 4(6), 736 – 744.
18. Tauc, J., Grigorovici, R., and Vancu, A. (1966). Optical Properties and Electronic Structure of Amorphous Germanium. *Phys. Status Solidi*, 15(2), 627 – 637.
19. Nwofe P.A. and Agbo P.E. (2015). Effect of Deposition Time on the Optical Properties of Cadmium Sulphide Thin Films, *International Journal of Thin Film Science and Technology* , Vol. 4, Iss. 2

20. Adelifard M. and Torkamani R (2015), influence of growth temperature and silver to sulfur molar ratios on optical, electrical and thermoelectrical properties of nanostructured Ag<sub>2</sub>S thin films, Journal of Materials Science: Materials in Electronics, Volume 26, pages 7554–7563

21. Pacheco-Salazar, Vilca-Huayhua, Paz-Corrales, Aragón, Mathpal L. Villegas-Lelovsky, J.A.H. Coaquira (2020), Growth and vacuum post-annealing effect on the structural, electrical and optical properties of Sn-doped In<sub>2</sub>O<sub>3</sub> thin films, Thin Solid Films, Volume 709, 1 September 2020, 138207

22. Jie Liang, Zhaoxue Yang, Lin Tang, Guangming Zeng, Man Yu (2017), Changes in heavy metal mobility and availability from contaminated wetland soil remediated with combined biochar-compost. Chemosphere, Volume 181, August 2017, Pages 281-288

UNDER PEER REVIEW